An agent-based model of a cutaneous leishmaniasis reservoir host, Meriones shawi

Wajdi Zaatour, Nicolas Marilleau, Patrick Giraudoux, Nadège Martiny, Abdesslem Ben Haj Amara, Slimane Ben Miled

An agent-based model of a cutaneous leishmaniasis reservoir host, *Meriones shawi*

Wajdi Zaatour[a,c], Nicolas Marilleau[f], Patrick Giraudoux[d], Nadège Martiny[e], Abdesslem Ben Haj Amara[b], Slimane Ben Miled[a]

[a]*Tunis El Manar University, Pasteur Institute of Tunis, laboratoire BIMS (LR16IPT09),* 1002, *Tunis, Tunisia*
[b]*University of Carthage, Carthage, Faculty of Science of Bizerte, Research Unit. Physics of Lamellar Materials and Hybrid Nannomaterials, Tunisia*
[c]*University of Carthage, Carthage, Faculty of Science of Bizerte, Tunisia*
[d] *Université de Bourgogne Franche-Comté/CNRS, Chrono-environment, 25030, Besançon, France*
[e]*Université Bourgogne Franche-Comté, Centre de Recherches de Climatologie/Biogéosciences, Dijon, France*
[f]*IRD/UPMC, UMI UMMISCO, 93143 Bondy, France*

Abstract

Meriones shawi (*M.shawi*) is the main reservoir host for zoonotic cutaneous leishmaniasis (ZCL) in Central Tunisia. The incorporation of environmental and climatic effects on the spread of ZCL in *M. shawi* remains difficult. This study presents an agent-based model (ABM) to overcome these difficulties and examine the impact of environment (*i.e.* vegetation cover) and climate (*i.e.* temperature) on *M. shawi* movement and prevalence. The model simulation considers two agents type: rodent agent and field unit agent. We tested the model according to two types of rodent movement: random and thoughtful. We integrated time dependent normalized difference vegetation index (NDVI) in order to test the land cover effects on rodent movement and ZCL transmission. The results confirmed that the spread of the disease depends on rodent movement. We observed that prevalence and distribution are the closest to field data when the vegetation cover is highest and that rodents go for thoughtful movement. In addition, we found that the nature of movement (random or thoughtful) and prevalence depends strongly on minimum food detection.

Keywords: Agent based model, Zoonotic cutaneous leishmaniasis, Meriones shawi, NDVI, Temperature

1. Introduction

Infectious diseases are a global public health problem. It is estimated that 75% of human infectious diseases originate from an animal reservoir and the majority are caused by viruses, bacteria, or parasites (Taylor et al., 2001). Among these diseases, leishmaniasis is predominantly observed, where 350 million people are at risk of contracting it and approximately 2 million new cases are reported each year (Arenas et al., 2017). Cutaneous leishmaniasis (CL) is a cutaneous infection caused by a unicellular parasite (*Leishmania*), transmitted by the bites of a female insect called phlebotome or sandfly (Dedet, 2009).

In Tunisia, zoonotic cutaneous leishmaniasis (ZCL) is caused by the parasite *Leishmania major* (*L. major*) (Ben Ismail et al., 1986), with its vector *Phlebotomus papatasi* (*P. papatasi*) (Killick-Kendrick, 1999). The latter's reservoir species include rodents *Psammomys* (*obesus*) (Cretzschmar, 1828), *Meriones* (*shawi*) (Duvernoy, 1842), and *Meriones* (*libycus*) (Lichtenstein, 1823).

The spatial dynamics of rodent populations involve several endogenous processes, such as the availability of food resources or exogenous processes such as environmental and climatic processes (Chaves and Hernandez, 2004; Bellali et al., 2017, 2019). According to the literature, *P. obesus* is known for its dietary restrictions, and feeds mainly on chenopodiaceae (Ghawar et al., 2011). It is considered a sedentary rodent with small home ranges (Daly and Daly, 1975; Ghawar et al., 2011). Furthermore, *M. shawi* is an opportunistic rodent that is able to adapt to its diet according to the development of cultivated cereals (Adamou-Djerbaoui et al., 2013); it is considered more mobile compared to *P. obesus* (Ghawar et al., 2015).

The Geographic Information System (GIS) data and machine learning are important for the management of epidemics because they allow the collection, analysis and display of epidemic spatiotemporal information (Tabasi and Alesheikh, 2019; Mollalo et al., 2018). These approaches were used to study the distribution of rodent reservoirs and sandfly.

In particular, the effect of the environment on the distribution of ZCL has extensively investigated. Various studies have been conducted to describe the niche suitability of vectors (Hanafi-Bojd et al., 2015), reservoirs (Gholamrezaei et al., 2016), or both (Shiravand et al., 2018, 2019) using the MaxEnt algorithm model. Particularly, (Hanafi-Bojd et al., 2015) proved that moisture, precipitation, and temperature are determining factors when assessing sandfly density. Furthermore, Bellali et al. (2017); Talmoudi et al. (2017) have shown a significant correlation between climate variables (precipitation and temperature) and the incidence of ZCL and rodent and sandfly density. One possible explanation for the latter ob-

servation is the correlation between that rodents and chenopodiaceous densities (Toumi et al., 2012).

Various deterministic models have already been developed for epidemics of leishmaniasis from different perspectives. Carpenter et al. (1992) and Burattini et al. (1998) developed structured models for canine leishmaniasis considering human and sandflies. Chaves and Hernandez (2004) presented a model for the dynamics of transmission of American Cutaneous Leishmaniasis. They obtained expressions that allow computing the threshold conditions for the persistence of the infection. Roy et al. (2015) used the same approach, but rather, considered the effect of the time lag between the biting of a sandfly and the human infection. In the other hand, Nadeem et al. (2019) proposed a mathematical model of ZCL concerning humans, reservoirs, and sandflies. They describe ZCL transmission and estimate the basic reproduction number R_0 using the next-generation matrix threshold condition. In addition, they tested different strategies to control the disease based on the indices of parameters.

Even though numerous studies were conducted on this topic, rarely those who considered the temperature as a factor influencing the ZCL transmission. Up to our knowledge, only Bacaër and Guernaoui (2006) and Mejhed et al. (2009) have integrated this factor in their deterministic models.

In all these mathematical models, the population and individual interactions are considered homogeneous. This assumption results in difficulties in representing the variants of individual microscopic attributes and behaviors and implicitly assumes that all individuals are subject to the same process (Duan et al., 2015; Hunter et al., 2018).

An agent-based model (ABM) is an integrative approach that takes into account the individual behavior diversity. The model is defined as a system comprising several entities or agents (*e.g.* individual) that operate in an environment, in which they are located. This agent is characterized by attributes, behaviors, capacities of perception, and communication (Treuil et al., 2008; Grignard, 2015). In this context, ABM makes it possible to represent and link different levels of detail, such as the effect of the spatial dynamics of the reservoir on the transmission of vector-borne diseases (Grimm et al., 2006) or the integration of the metapopulation model in the context of rodent dynamics (Marilleau et al., 2018).

Rajabi et al. (2016) used an ABM with two types of agents, which are the sandfly and the human in a structured environment (road, land cover, river,...), knowing that the infection probability depends on the environmental. They were able to confirm that desertification zones are the main source of ZCL and local populations are the most exposed to sandflies.

Recently, Rajabi et al. (2018) used an ABM to simulate authority interventions on *Rhombomys opimus* (rodent reservoir of ZCL in Iran) population, to minimize ZCL incidence. They showed the impact of habitat configurations and human-made changes on rodent communities and their dynamics.

More recently, Tabasi et al. (2020) used an ABM to represent the complete cycle of ZCL disease, *i.e.* human, sandfly, rodent, and environmental behaviors using an hybrid model. They showed that the spread of ZCL is important in some regions like the desert, low altitude areas, and, riverside population centers. They also confirmed that restricted human movement is an important factor contributing to the reduction of transmission frequency .

In our study, we developed an ABM to determine how the rodents (*i.e. M. shawi*) movement types can affect transmission ZCL transmission taking into account time dependent environmental (*i.e.* vegetation cover) and climate constraints (*i.e.* temperature). Indeed, we assumed that vegetation cover is updated each month using NDVI values and may vary depending on rodent consumption. In addition, we supposed that rodents decisions (*e.g.* decision to move, choice of directions ...) are affected by the vegetation cover (Mollalo et al., 2014; Ghawar et al., 2015). We simulated two types of rodents movement, a random movement and a so-called "thoughtful" movement, where rodents can choose their direction after evaluating the state of vegetation based on their memories. In addition, we have tested NDVI effects on the transmission of the epidemic.

In Section 2, we present the background and hypothesis used in the model. In Section 3, we describe the model according to the Overview, Design concepts, and Details (ODD) protocol (Grimm et al., 2010) to standardize its description. In Section 4, we present the main results. In Section 5, we discuss our results. Finally, in Section 6, we present the conclusion of our work.

2. Background

Climatic and environmental factors impact rodents distribution (Hamidi et al., 2018). In fact, the rodents reproductive cycle is indirectly influenced by climatic conditions as the latter influence such as the resource availability (Stenseth, 1999, 2003). Marstona et al. (2007) and Chidodo et al. (2020) showed a correlation between vegetation cover and rodent distribution. When the resource is abundant, rodents tend to be close to foraging areas. Otherwise, their movement is random when the food became rare (Ghawar et al., 2015). This is probably resulting from rodents ability to assess to food through the information they have on the occupied area.

At the vector level, sandflies are characterized as thermophilic, requiring high temperatures for their development and survival (Koch et al., 2017) (see Fig. 1).

At the parasite level (*L.major*), an increase in temperature increases the rate at which parasites approach maturity and multiply, which promotes transmission of the infection (Clémence, 2009). However, when the parasite is in the intestine of infected sandflies, it remains at the same temperature as his host (Zilberstein and Shapira, 1994), which considered as the environment temperature (see Fig. 1).

Considering temperature or humidity explicitly in the population dynamics model through the sandfly life cycle is difficult. To overcome this, we assumed that there is a positive correlation between NDVI and temperature on the one hand (Wang et al., 2003), and infection probability, on the other (Mollalo et al., 2014; Shiravand et al., 2018). More precisely, we suppose that the ZCL infection probability depends linearly on the sandfly density, which depends on temperature via a bell-like function. The height of the bell depends on NDVI. This hypothesis is not meaningless as Mollalo et al. (2015); Garni et al. (2014); Shiravand et al. (2018) developed a model to discuss the associations between NDVI and the incidence of cutaneous leishmaniasis.

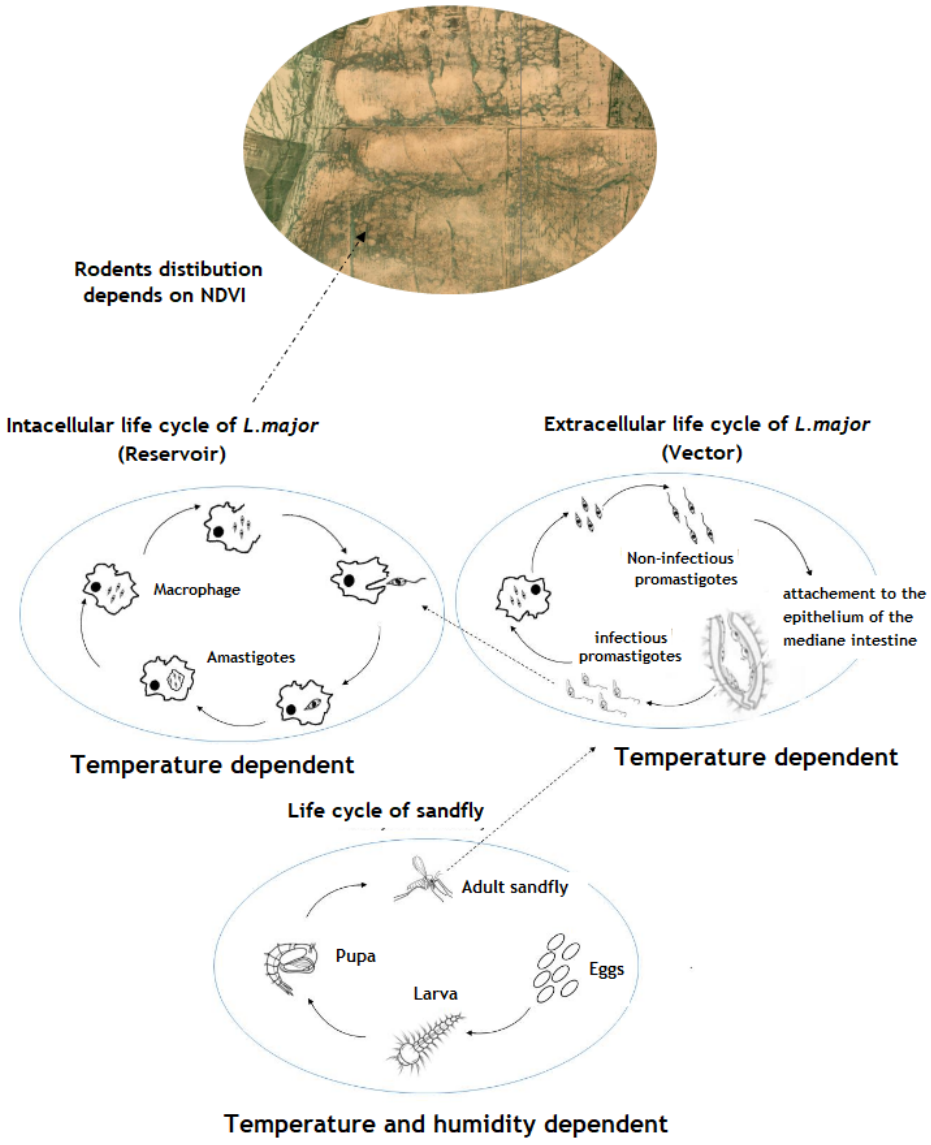

Figure 1: Cycle life of *L.major* and factors influencing sandfly and rodent.

Therefore, temperature and NDVI can be considered as good proxies for the presence probability of both vectors and reservoirs (Shiravand et al., 2018).

Our study presents a simulation of *M. shawi* activity in a spatially heterogeneous environment, incorporating individual-based interactions. We used empirical data on rodents and their habitat and ZCL incidence in El Manara region (average altitude $80, 8483$ m; lat $35°12'36"$N, Long $9°49'14"$E) in Nasrallah, Kairouan, Central Tunisia (see Fig. 2). The area is a semiarid plain located at an altitude of $205, 1304$ m and is composed of *Arthrophytum sp.*, *Retama sp.*, *Ziziphus mound*, and *Opuntia hedges* (Ghawar et al., 2011). Additionally, El Manara has long been known as one of the most important endemic areas of ZCL (Bettaieb et al., 2014), and *M. shawi* is the main reservoir host of ZCL in this area. The annual incidence rate in Kairouan has been high in recent decades, including approximately $34.4/100,000$ inhabits, and the disease has recently emerged in non-endemic regions of the province (Chraiet-Rezgani et al., 2016). Our model does not incorporate humans as agents. However, human-induced changes are included to explore the consequences of disease evolution among rodent population dynamics. As such, the model can be a useful tool for informing healthcare authorities in planning intervention strategies to control the spread of ZCL.

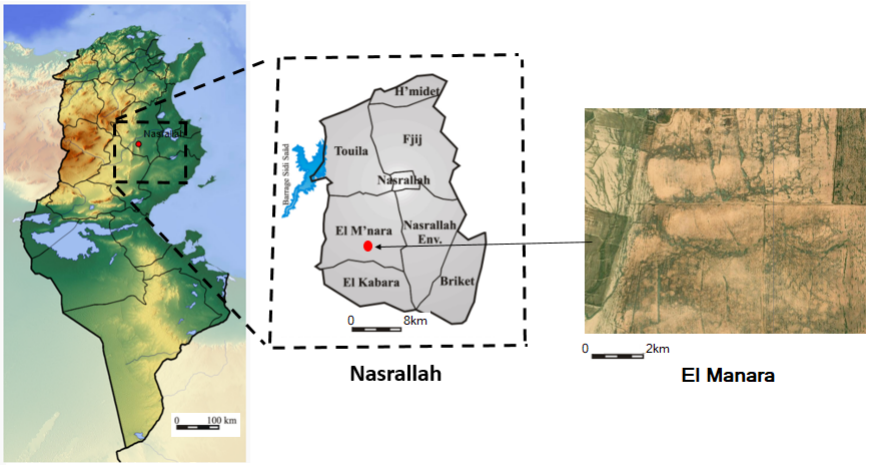

Figure 2: Study area at EL Manara, Nasrallah, Kairouan governorate.

3. The model

The model description follows ODD protocol for describing agent-based models (Grimm et al., 2010). In the remainder of this section and after a brief overview of the model components and process (see subsection 3.1), the key concepts of

model design, including emergence, objective, sensing, adaptation, stochasticity, and observation , are described (see subsection 3.2). Next, the details of the model implementation are presented (see subsection 3.3).

3.1. Overview

Our main objective is to design a spatial ABM of the ZCL spread among rodents, including environmental and climatic data and agent objects. The model was developed in the GAMA 1.7 platform (Taillandier et al., 2019).

3.1.1. Purpose

The model was developed to provide a spatiotemporal simulation of the spread of ZCL between rodents (*M. shawi*). We assumed two types of movement: random and thoughtful. The thoughtful movement depends on the vegetation density where the rodent is able to evaluate the "best" destination. The model includes climatic factors (e.g., temperature), and environmental (e.g., NDVI) factors influence the movement and spread of the ZCL between rodents.

3.1.2. Entity, state variables, and scales

There are two types of agents in the model, rodent agent and field unit agent representing part of the space (see Fig. 3).

The rodent agents : They are described by their identifier, position, and epidemiological status concerning ZCL (susceptible or infected) and by two matrices M_{info} and M_{food} (see Table 1) .

The field unit agents : They form the grid and represent the environment of the ABM. They are attributed by their identifier and by F_{cell}, representing the quantity of food present in the cell, it changes according to the quantity consumed by the rodent agent and is updated each month according to the integrated NDVI values. The grid contains 1530 field units (the area of each unit is $895\ m^2$), and its surface is $1.37\ km^2$. The choice of the value is based on our observations on the field for a project to be conducted in 2012 (Ghawar et al., 2015).

Regarding temporal resolution, the time step of the simulation was fixed to 1 h. The model has been designed to perform simulations for up to 5 years.

Table 1: Summary of attributes and variables with definitions. In the description of the dimensions, the following symbols are used: $-$ indicates no dimensions, J: Joule, t: time.

Agent	Symbol	Type	Description	Unit	Update period
Rodent	R_{xy}	**Point**	Position of the rodent agent	$-$	1 hour
	AF_{consum}	$\mathbb{R}$	Speed of food consumption made by the rodent agent at each step of the time	$J.t^{-}1$	1 hour
	AF_{min}	$\mathbb{R}$	Minimum quantity of food detected by the rodent agent to move	J	1 hour
	q	$\mathbb{R}$	Quantity of food consumed by rodent agent	J	1 hour
	L_{memory}	$\mathbb{R}$	Loss memory rate	$t^{-}1$	1 hour
	M_{info}	**Matrix**	Matrix containing information about the presence of food. Its values are between 0 (no information) and 1 (complete information). The size of the matrix corresponds to that of the environment (1530 cells)	$-$	1 hour
	M_{food}	**Matrix**	Matrix containing the perception of the food values of each cell. The size of the matrix corresponds to that of the environment (1530 cells)	J	1 hour
	V_{min}	$\mathbb{R}$	Minimum forward term product of the two matrices M_{info} and M_{food}	J	**Fixed**
	p	$\mathbb{R}$	Infection probability, which depends on temperature and NDVI	$-$	1 month
	γ	$\mathbb{R}$	Recovery probability	$-$	1 week
	α	$\mathbb{R}$	Infection factor	$-$	**Fixed**
Field unit	F_{xy}	**Point**	Position of the field unit agent	$-$	**Fixed**
	F_{cell}	$\mathbb{R}$	Quantity of food present in each field unit	J	1 hour

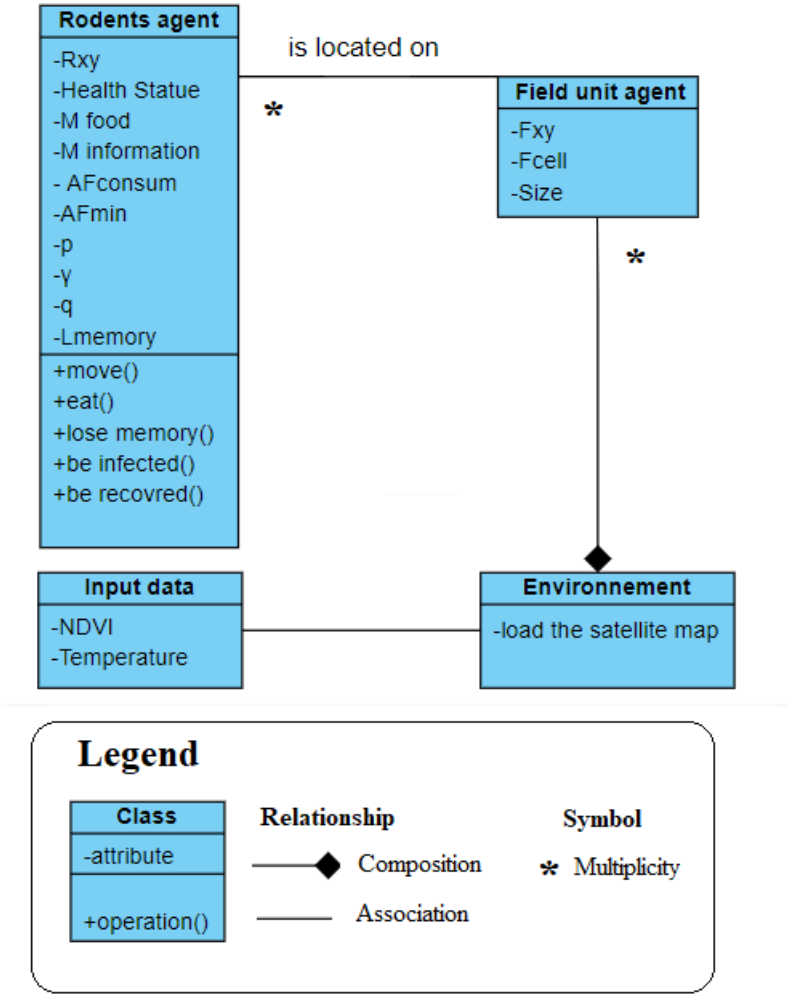

Figure 3: UML (unified modeling language) class diagram represents our ABM, there are two types of agents: rodent agent and field unit agent. Rodent agents are located in field units.

3.1.3. Process overview and scheduling

The simulation time-step represents one hour. Except for the recovery process, which is operated every week.

Rodent agent: First, rodent agents appear in the landscape at different random locations. Then, rodent agents are processed using the consumption process under particular conditions. When the quantity of food becomes insufficient, the rodent

agents choose a destination and move to another cell. Then, the matrix-update process is activated. Subsequently, the memory loss process is operated (see Fig. 4).

Field unit agent: First, the field unit values are updated according to the environmental parameters (NDVI). At each time step, the values of the quantity of food decrease according to the number of rodent agents present in the cell and their consumption speed AF_{consum}. At each month, the field unit values are re-updated according to the values of the integrated NDVI. The model simulates the interactions between rodent agents on the one hand and between rodent agents and field unit agents on the other hand over time. The infected agent rodents perceive susceptible rodents in the same cell. Then, the infection process is activated. Subsequently, and at each week, the recovery process is performed (see Fig. 5 and 6).

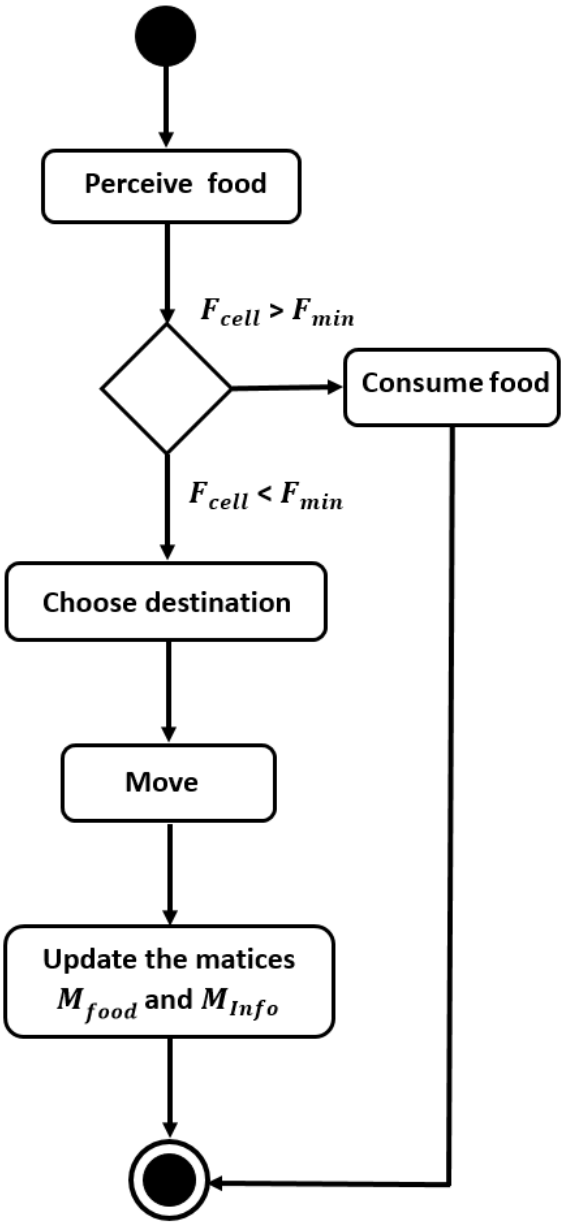

Figure 4: Conceptual view of movement, consumption, and update matrices: the diagram represents an outline of the sequence of processes and the schedule of interactions between agents at each discrete time step.

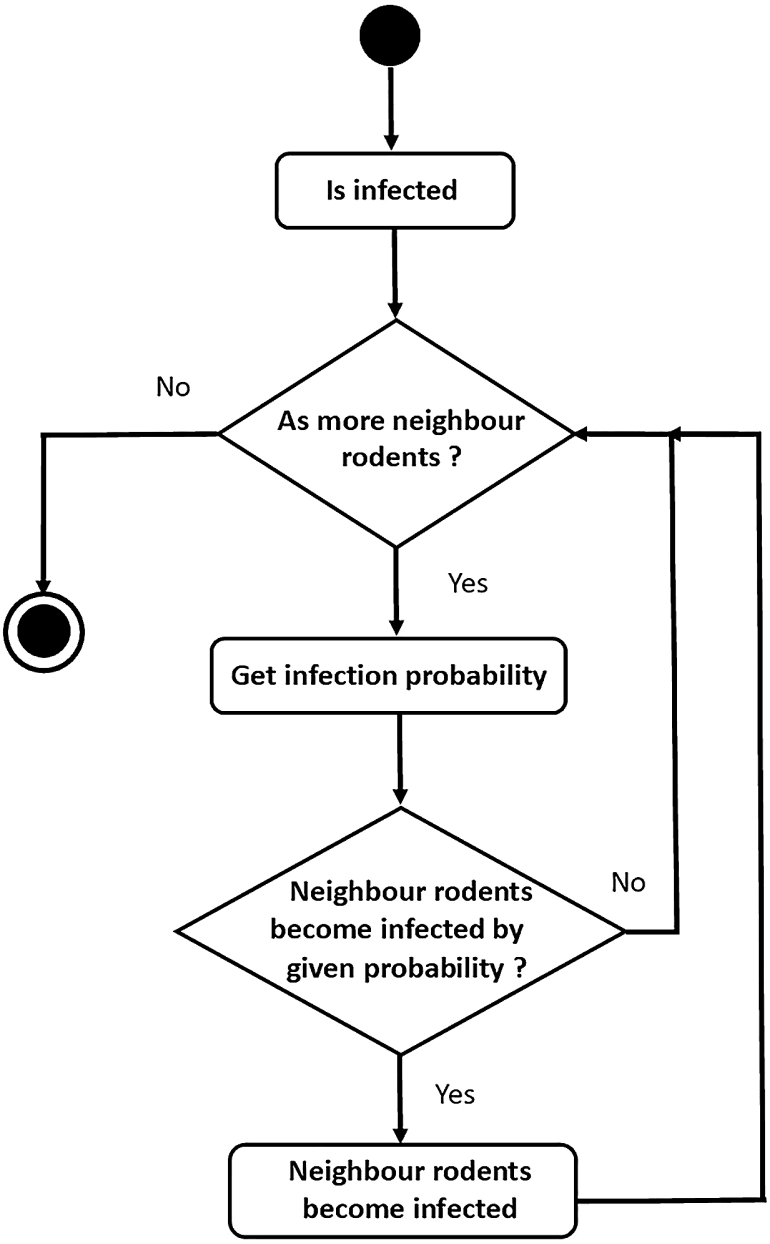

Figure 5: Conceptual view of the infection process (it is activated each time step).

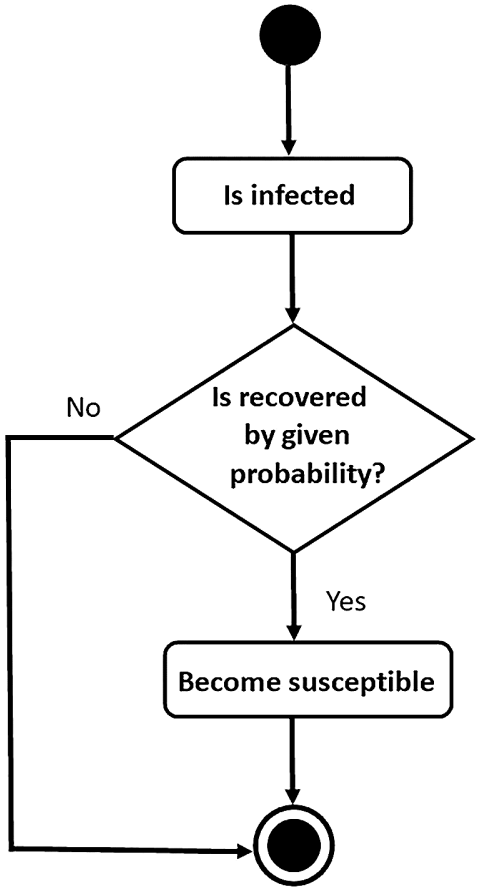

Figure 6: Conceptual view of the recovery process (it is activated each week).

3.2. Design concepts

3.2.1. Emergence

Depending on the evolution of F_{cell}, we observe a spread of the epidemic that takes into account the mobility, interactions and, characteristics of the rodent agents.

3.2.2. Objective

The objective of the agent is to find and consume food. The way to find food depends on the type of rodents movement (random or thoughtful).

3.2.3. Sensing

Rodent agents know how to identify suitable habitats within the environment, and they perceive the cell information status from M_{food}. In addition, they can perceive other rodent agents located in the same field unit.

3.2.4. Adaptation

The agents adapt their type of movement (random or thoughtful) to the amount of food in cells. This adaptation depends on the value of minimum food detection AF_{min}.

3.2.5. Stochasticity

The agents move randomly through space by one spatial unit (e.g., grid cells), and they choose one of the cells in the proximity. The infection probability follows a Gaussian law. In the recovery process, the agent choice of the direction all includes elements of stochasticity.

3.2.6. Observation

Spatiotemporal variations in the rodent-level process have been observed in the model. These included the number of susceptible and infected rodents at each step of the time. We also monitored the number of times the rodent agents passed through each agent cell. Moreover, at the end of each simulation, we reported the infected density (prevalence) as $P = \frac{N_{inf}}{N_0}$, and the susceptible density noted $S = \frac{N_s}{N_0}$, N_{inf} is the number of infected rodent agents, N_s is the number of susceptible rodents, and N_0 is the total number of rodent agents.

We also report the entropy H of the occupied site distribution. We assumed that the random variable $X = (X_1, \ldots, X_m)$, where X_i is "the number of times the site $i \leq m$ is visited" random variable follows a multinomial distribution of parameter $(N, p_1, ..., p_m)$, where m is the site number ($m = 1531$), $X_1 + ... + X_m = N$, N is the total number of rodent movements, and p_i, $i \leq m$ is the probability that a rodent has occupied site i, we have $\sum_{i=1}^{m} p_i = 1$. Therefore, we have:

$$f(x_1, \ldots, x_k; n, p_1, \ldots, p_k) = \Pr(X_1 = x_1 \text{ and } \ldots \text{ and } X_k = x_k), \tag{1}$$

$$= \begin{cases} \dfrac{N!}{x_1! \cdots x_k!} p_1^{x_1} \cdots p_k^{x_k}, & \text{when } \sum_{i=1}^{k} x_i = N \\ 0 & \text{otherwise,} \end{cases} \tag{2}$$

In the case where sites are chosen equiprobably - *e.g.* no food on site and rodents have no sensory organs or memory and move randomly, the law is an equi-distributed multinomial and $p_i = p = 1/m$. We have:

$$f(x_1, \ldots, x_k; n, p, \ldots, p) = \Pr(X_1 = x_1 \text{ and } \ldots \text{ and } X_k = x_k), \tag{3}$$

$$= \begin{cases} \dfrac{N!}{x_1! \cdots x_k!} p^N, & \text{when } \sum_{i=1}^{k} x_i = N \\ 0 & \text{otherwise,} \end{cases} \tag{4}$$

To evaluate the values of p_i, and as each simulation has a different total number of movements, we normalize N to 5000. A good estimator of p_i is $\tilde{p}_i = N_i/N$, where N_i is the normalized number of site visits i calculated from either field observation data or simulation data.

3.3. Details

3.3.1. Initialization

50 rodents were randomly created throughout the environment with a susceptible status. Only one infected rodent were randomly selected; the initial values of M_{food} and M_{info} were 0. Table 2 represents the model initialization parameters.

Table 2: Parameters and input values of the rodent agent and field unit agent. In the description of the dimensions, the following symbols are used: $-$ indicates no dimensions, J: Joule, t:Time, A: Authors' estimation, E: Experts' judgments.

Symbol	**Default value**	**Range**	**Unit**	**Source**
N_0	50	**Fixed**	$-$	**A**
N_{inf}	1	**Fixed**	$-$	**A**
γ	0.001	$0.009 - 0.011$	$-$	**E**
α	1	$0.9 - 1.1$	$-$	**A**
AF_{consum}	0.001	$0.009 - 0.011$	$J.t^{-}1$	**E**
L_{memory}	0.8	$0.79 - 0.81$	$t^{-}1$	**E**
AF_{min}	$\{0.2; 0.7\}$	$0.19 - 0.21$	J	**A**
V_{min}	0.0001	**Fixed**	J	**A**

3.3.2. Input Data

At the beginning of each month, a satellite map is included containing the NDVI values of each cell, representing the amount of resources produced. The

maps (with a surface area of $1.37\ km^2$) were downloaded for each month using the $Landsat\ 8$ sensor (30 m resolution), and processed in ArcGis 10.3. We calculated the monthly NDVI values for each cell (between 0 and 1). To test their effects on the model simulation, we integrated three types of NDVI:

- $NDVI_{max}$: These are the maximum monthly values of the NDVI (collected on 2014) whose plant density is considered the highest.
- $NDVI_{mean}$: These are the average monthly values of the NDVI between 2013 and 2017.
- $NDVI_{min}$: These are the minimum monthly values of the NDVI (collected on 2015) whose plant density is considered the lowest.

Average monthly temperatures were obtained from a weather forecasting station that was implemented in the study area in 2012 (data not shown).

3.3.3. Submodels

Consumption submodel. If F_{cell} is $\geq AF_{min}$, the rodent agent consumes food with a consumption rate of AF_{consum}. The variation in food quantity F_{cell} is governed by the following equation:

$$F_{cell}(t + \delta t) = F_{cell}(t) - \min(F_{cell}, AF_{consum}) \tag{5}$$

Matrices update process:. For each time step, the following algorithm, which describes the matrices update, is run :

Algorithm 1 Algorithm represents the update of M_{food} and M_{info}. For each field unit i, we note that (i_x, i_y) for the coordinates in the matrix M_{food} and M_{info} associated with i. We recall that M_{food} is the matrix containing information about the presence of food and M_{info} is the matrix containing the perception of the food values of each $cell$, both have the same dimension as field units. $Neighb(i)$ represents the neighboring field unit i. $MyCell$: is the field unit where agent rodents are.

$M_{info}(MyCell_x, MyCell_y) \leftarrow 1$
if $F_{cell}(MyCell) > F_{min}$ **then**
  $M_{food}(MyCell_x, MyCell_y) \leftarrow F_{cell}(MyCell)$
else
  $M_{food}(MyCell_x, MyCell_y) \leftarrow 0$
end if
$Minformation \leftarrow M_{info}$
$Mfood \leftarrow M_{food}$
for i in $Neighb(MyCell)$ **do**
  $Minfo(i_x, i_y) \leftarrow \max(mean_{k \in Neighb(i)}(M_{info}(k_x, k_y)), M_{info}(i_x, i_y))$
  if $M_{info}(i_x, i_y) \neq 1$ **then**
    $Mfood(i_x, i_y) \leftarrow mean_{k \in Neighb(i)}(M_{food}(k_x, k_y))$
  end if
end for
$M_{info} \leftarrow Minformation$
$M_{food} \leftarrow Mfood$

Movement submodel. We performed the two scenarios of movement by setting parameters that affect the type of movement (random versus thoughtful) AF_{consum}, AF_{min}, and L_{memory}. Two different dispersal behaviors were identified:

- Random: The rodent agent moves cell by cell. From a cell, the rodent randomly chooses the next neighboring cells. This behavior is applied to each agent at each step when AF_{min} is high (AF_{min} = 0.7). In this case, the minimum quantity of food that the agent must detect (in order to move) is greater than that available in neighboring cells, so the rodent moves randomly.

- Thoughtful: The rodent agent makes a selection of a neighboring cell. This choice is made with regard to the values of M_{food} and M_{info}. Rodent moves according to the information collected on the vegetation status of neighboring cells. The cell chosen is the one that maximizes the forward term prod-

uct of the two matrices M_{info} and M_{food}. If this maximum is less than a certain value previously set (noted V_{min}), the movement will be random.

Memory loss submodel. In the model, we assumed that the rodent agent can forget information about a cell that has visited before. For this purpose, the values of the M_{food} matrix are multiplied by a previously set rate, L_{memory}.

Infection submodel. At every step, susceptible rodent agents can be contaminated with an infection probability p that depends on the temperature and NDVI, since these two factors have an impact on the transmission of the epidemic. p follows a Gaussian law based on the assumption that plants grow if the temperature increases, except that above a set value, plant density decreases. On the other hand, we supposed that each susceptible agent observes at the infected agents in its proximity at a distance of $R_{infection}$ (set at 0), we assumed that the transmission of the epidemic can only occur if a susceptible and an infected agent occupy the same cell.

$$p = \frac{\alpha(\text{NDVI})}{\sigma\sqrt{2\pi}} \exp\left(\frac{-(T - T_{optimal})^2}{2\sigma^2}\right) \tag{6}$$

where $\sigma = \sqrt{\frac{(T_{max}-T_{optimal})^2+(T_{min}-T_{optimal})^2}{2}}$, T is the field temperature, $T_{optimal}$ is the average temperature, T_{max} is the maximum temperature, T_{min} is the minimum temperature and α is the infection factor.

Recovery submodel. At the end of each week, infected rodents can be recovered with a fixed recovery probability γ.

Food evolution submodel. The evolution of F_{cell} is related to the values of the integrated NDVI, which represents the initial quantity of food (at the beginning of each month F_{cell} = NDVI). NDVI is integrated in the form of a monthly satellite map of the EL Manara region. These images provide us with information on the vegetation status of the field. This process is operated every month; once the consumption process is activated, F_{cell} decreases with the agent consumption.

4. Results

Simulations were performed using the Gama $1.7.0$ platform to develop the agent-based simulator Python 3 to generate the experiment plan and sensitivity analysis.

To see the movement effect (i.e., random or thoughtful) and the NDVI choice (i.e., $NDVI_{min}$, $NDVI_{mean}$, and $NDVI_{max}$) on the spread of the epidemic (i.e.,

the infected versus susceptible rodents), we performed a simulation of 50 agents over 5 years. Each simulation was repeated 30 times. We have represented on Fig. 7 and Fig. 8 the average of infected density and susceptible density on the simulations. In the thoughtful movement, we set $AF_{consum} = 0.001$, $AF_{min} = 0.2$, and $L_{memory} = 0.8$. However, to obtain a random movement, we fixed $AF_{min} = 0.7$.

We tested the model using an exhaustive method that consists all the possible combinations of the parameters (basic and modified) and reviewing those that give prevalence close to that of reality. To the best of our knowledge, there is only one study in Central Tunisia that demonstrated the prevalence of *L. major* infection among *M. shawi* rodents (Ghawar et al., 2011). The prevalence of *L. major* for indirect fluorescent antibody test was 0.33.

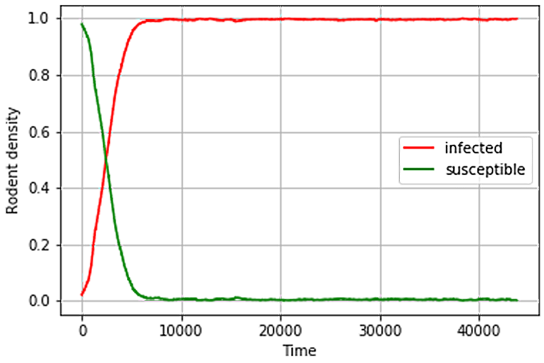

(a) NDVImax

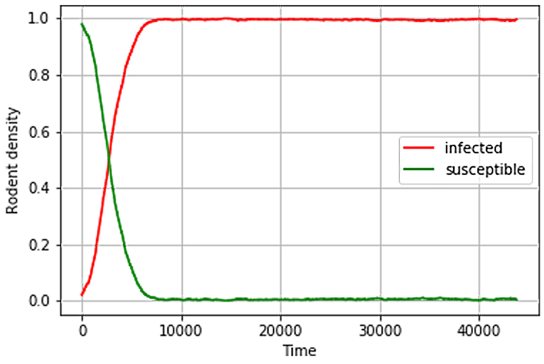

(b) NDVImean

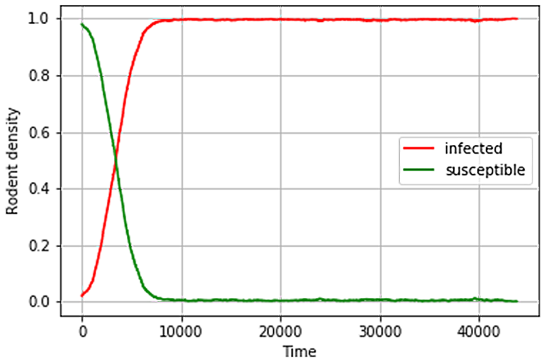

(c) NDVImin

Figure 7: Figures representing the dynamics of infected rodents (red curve) and susceptible rodents (green curve) with varying NDVI in random movement case.

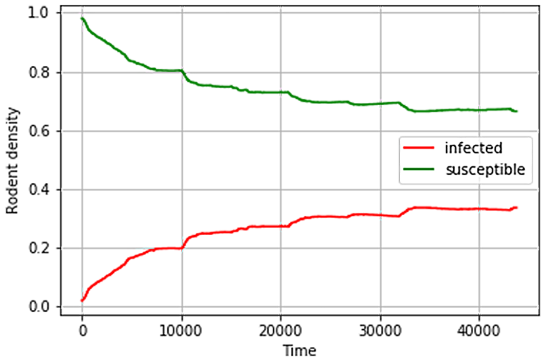

(a) NDVImax

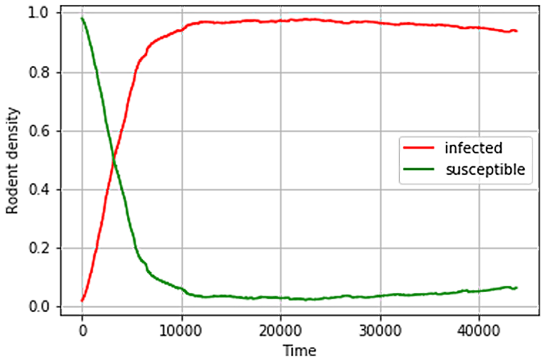

(b) NDVImean

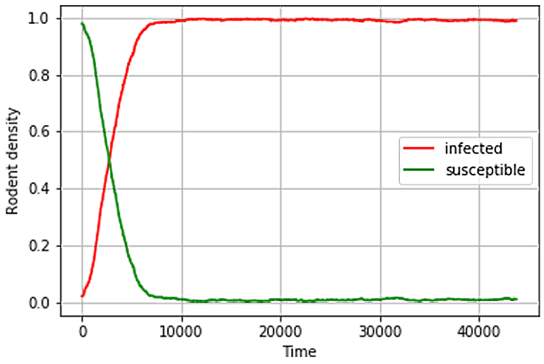

(c) NDVImin

Figure 8: Figures representing the dynamics of infected rodents (red curve) and susceptible rodents (green curve) with varying NDVI in thoughtful movement case.

We noted that the type of movement affects the variation in infected density. In the random movement case, all rodents become infected (see Fig. 7). The same behavior can also be observed in the case of $NDVI_{min}$ when the movement is thoughtful (Fig. 8c). In the $NDVI_{mean}$ case (thoughtful movement), the majority of rodents are infected (between 94% and 98%). We also observed a slight decrease in the infected density over the last 2 years (see Fig. 8b). In $NDVI_{max}$ case when the movement is thoughtful (Fig. 8a), there is a small increase in the infected density with a stability at the end of the simulation (30% of rodents are infected).

We calculated the average prevalence (in the last 3 years) that $\overline{P_{max}}$, $\overline{P_{mean}}$, and $\overline{P_{min}}$ (corresponding to $NDVI_{max}$, $NDVI_{mean}$, and $NDVI_{min}$, respectively). It can be seen that they are greater in the first scenario (random movement). Thus, we noticed that the average prevalence is inversely proportional to the NDVI values in the case of thoughtful movement (see Table 3).

Table 3: Mean prevalence and standard deviation (SD) values calculated over the last 3 years.

Type of movement	**Type of prevalence**	**Value of prevalence**	**SD**
Random	$\overline{P}_{max}$	0.99	0.06
	$\overline{P}_{mean}$	0.99	0.06
	$\overline{P}_{min}$	0.99	0.06
Thoughtful	$\overline{P}_{max}$	0.34	0.006
	$\overline{P}_{mean}$	0.92	0.01
	$\overline{P}_{min}$	0.99	0.006

To examine the distribution of rodents in the cells and compare them with those in the field, we calculated the entropies noted H^r_{max}, H^r_{mean}, and H^r_{min} corresponding to the first scenario (random movement) and H^{th}_{max}, H^{th}_{mean}, and H^{th}_{min} corresponding to the second scenario (thoughtful movement). We calculated the entropy ratio $r = \frac{H}{H_{field}}$ (H_{field} is the entropy of the real distribution of rodents in the field) to compare the model entropies and field data (Fig. 9).

The results showed that when the movement is random, the entropy ratio is almost equal to the maximum entropy ratio $r_{uniform}$ (the most disordered state). Moreover, we noted that when the movement is thoughtful, the entropy ratio is close to that of the field. The value of the entropy ratio closest to that of the field is in the case of NDVI = $NDVI_{max}$, and it has been noted that if the simulation time is greater, the ratio entropy r^{th}_{max} is close to the value 1 (r_{field}).

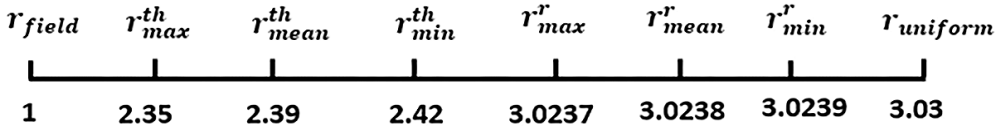

Figure 9: The entropy ratios: All entropies are normalized with respect to the field entropy H_{field}, $r_{field} = \frac{H_{field}}{H_{field}} = 1$, $r^{th}_{max} = \frac{H^{th}_{max}}{H_{field}}$, $r^{th}_{mean} = \frac{H^{th}_{mean}}{H_{field}}$, $r^{th}_{min} = \frac{H^{th}_{min}}{H_{field}}$, $r^{th}_{max} = \frac{H^{r}_{max}}{H_{field}}$, $r^{r}_{mean} = \frac{H^{r}_{mean}}{H_{field}}$, $r^{r}_{min} = \frac{H^{r}_{min}}{H_{field}}$, $r_{uniform} = \frac{H_{uniform}}{H_{field}}$. $H_{uniform}$ denotes the uniform distribution entropy. In the description of the entropy ratios, the following symbols are used: r: random movement, th: thoughtful movement, max: $NDVI_{max}$, mean: $NDVI_{mean}$ and min: $NDVI_{min}$.

Finally, we performed a sensitivity analysis to determine the parameters that could influence the prevalence. This analysis was applied in the thoughtful movement case when the NDVI was maximum. Thus, we used the one-factor-at-a-time (Cariboni et al., 2007; Saltelli et al., 2008) sensitivity analysis method that consists of selecting a base parameter setting and varying one parameter by $\pm 10\%$ at a time while keeping all other parameters fixed. Each simulation was repeated 30 times. The infection factor α, recovery probability γ, consumption rate AF_{consum}, minimum food detected AF_{min}, and loss memory rate L_{memory} parameters were tested.

Fig. 10 shows the variations in prevalence and standard deviation according to the modified parameters. In addition, a linear regression analysis was performed for each case. We estimated the coefficient of determination, slope, and intercept for each curve (Table 4)

The results show the effect of seasonality on the variation in prevalence and standard deviation. In addition, we noted that practically all the curves have the same slope, which is very low (in the order of 10^{-4}). This weakness can be explained by the stability of prevalence in the last 3 years.

In addition, we noted the impact of the parameters on prevalence and SD values. For example, in Fig. 10c, when the recovery probability γ is high, the prevalence value becomes lower. In the figure, when AF_{consum} is high, the prevalence value increases.

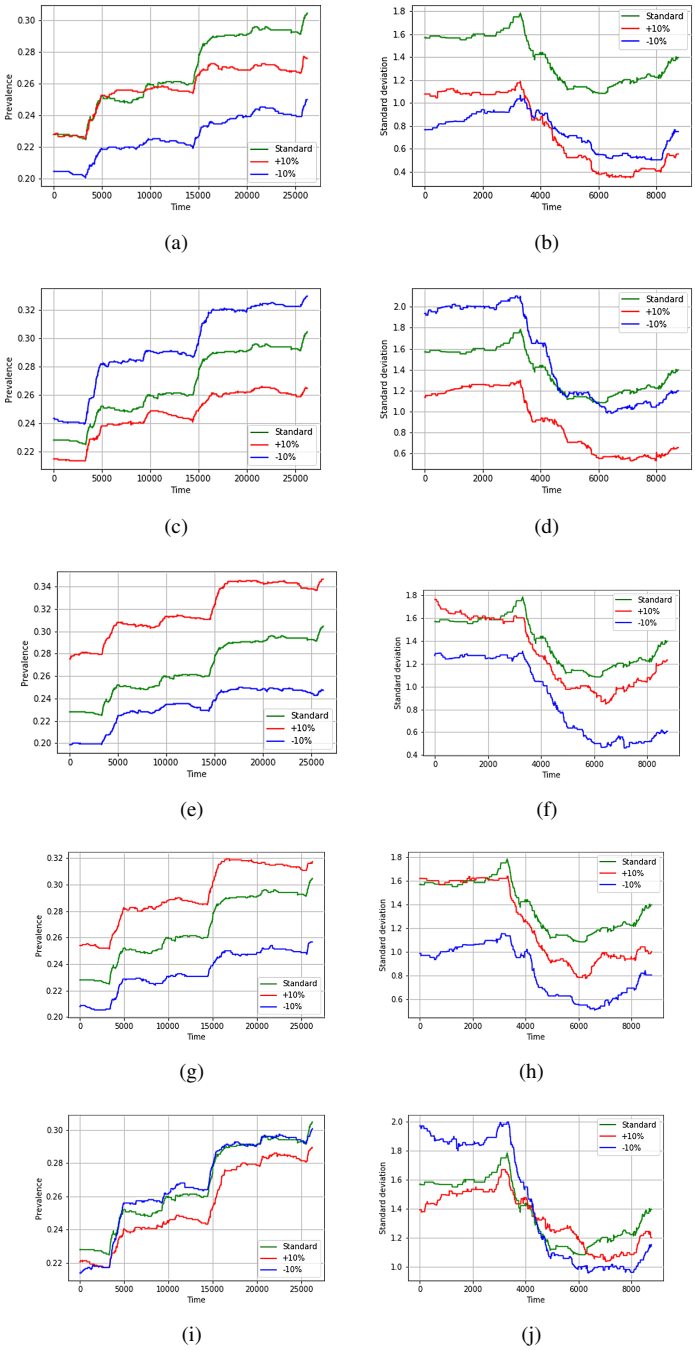

Figure 10: Figures (a), (c), (e), (g), and (i) represent the prevalence for different values of parameters α, γ, AF_{min}, AF_{consum}, and L_{memory} respectively. Figures (b), (d), (f), (h), and (j) represent SD for different values of α, γ, AF_{min}, AF_{consum}, and L_{memory}, respectively

Table 4: Coefficient of determination, slope, and intercept of linear regression line for each modified parameter. In the case of based parameters, R^2 = 0.93, slope = 10^{-4}, and intercept = 11.33

Parameter	Variation	Coefficient of determination	Slope	Intercept
α	$+10\%$	0.79	8.10^{-5}	11.74
	-10%	0.92	8.10^{-5}	10.23
γ	$+10\%$	0.85	9.10^{-5}	11
	-10%	0.88	10^{-4}	12.46
AF_{consum}	$+10\%$	0.85	10^{-4}	12.88
	-10%	0.88	9.10^{-5}	10.48
AF_{min}	$+10\%$	0.86	10^{-4}	14.12
	-10%	0.8	10^{-4}	10.34
L_{memory}	$+10\%$	0.88	10^{-4}	11.25
	-10%	0.93	10^{-4}	10.82

We then performed a sensitivity analysis to determine the effect of the 5 parameters on the mean prevalence over the last 3 years. We observe that the minimum food detected AF_{min} has a major effect on the mean prevalence, which increases by 0.2. The minimum food detected, AF_{min}, and the loss memory rate L_{memory} have a positive effect ; however, the recovery probability γ has a negative effect. (see Fig. 11a and Fig. 11b).

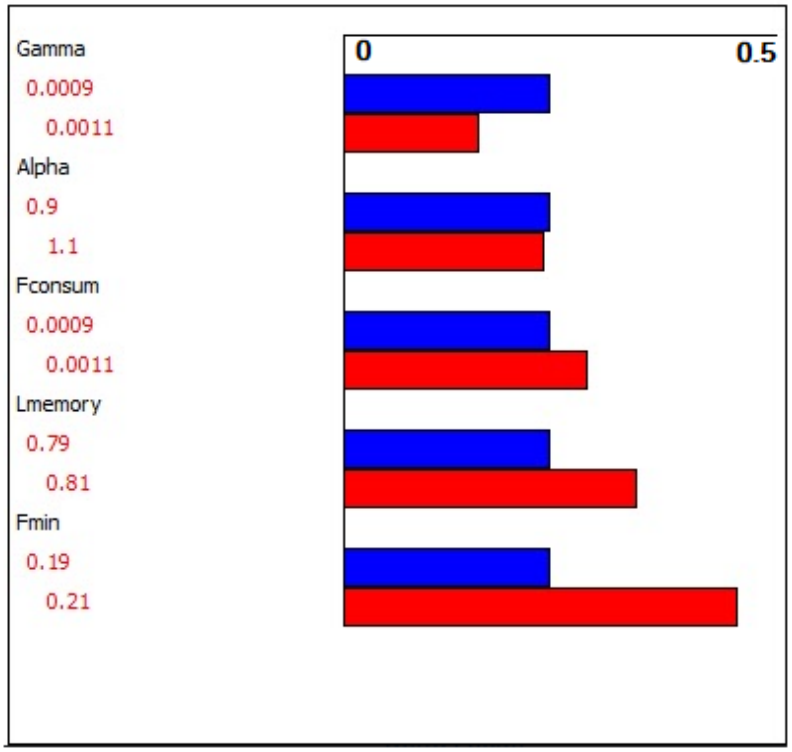

(a)

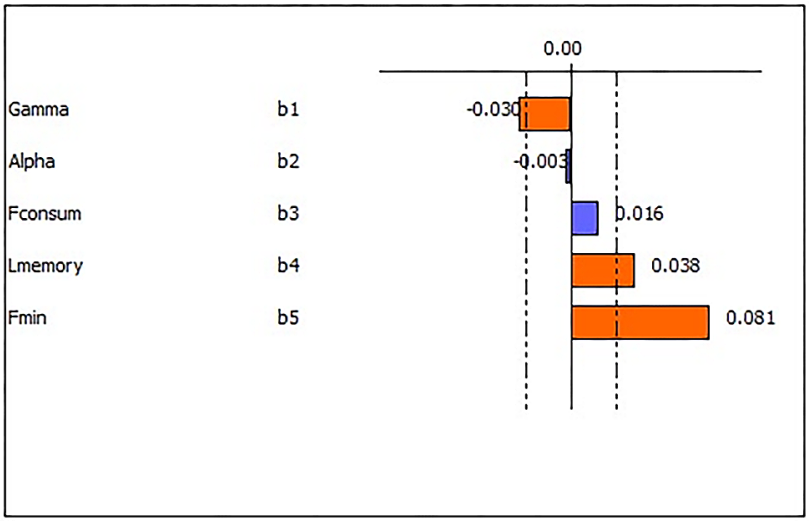

(b)

Figure 11: Factors influencing the mean prevalence

Table 5: Screening parameters for the mean prevalence. b_i correspond to the model regression coefficients. $\overline{Y} = b_0 + b_1\ \gamma + b_1\ \alpha + b_3\ AF_{consum} + b_4\ L_{memory} + b_5\ AF_{min}$.

Parameter	Coefficient	Value	Inflation factor	SD
	b_0	0.2808	1	0.0062
γ	b_1	-0.0301	1	0.0062
α	b_2	-0.0027	1	0.0062
AF_{consum}	b_3	0.0162	1	0.0062
L_{memory}	b_4	0.0380	1	0.0062
AF_{min}	b_5	0.0814	1	0.0062

5. Discussion

Our results highlight the importance of considering the type of movement (random or thoughtful) of reservoir rodents considering their influence on the transmission of the epidemic. In the first scenario (random movement), the prevalence values were higher than those in the second scenario. This difference can be explained by the activity of rodents who forage randomly. The fact that the movement is random implies that the probability of an encounter is a product of the frequencies of the infected and susceptible rodents (i.e., mass action law). Thus, in this case, our model is "close" to an SIS model (susceptible-infected-susceptible epidemiological model). The term "close" refers to the fact that rodents spend the maximum of their time foraging *i.e.* , the case where $NDVI = NDVI_{mean}$ and $NDVI = NDVI_{min}$. In the case where $NDVI = NDVI_{max}$, the fluctuations may be due to the fact that rodents spend more time consuming food; thus, there is a lower possibility of being infected.

In the second scenario, when rodents accessed food more rapidly, the risk of infection was reduced because the probability of an encounter was lower. This explanation is supported by the fact that in the case where NDVI is weak (i.e., $NDVI = NDVI_{min}$), the number of infected rodents becomes high again. If food is scarce, the information on feeding sites is low; therefore, the rodents adopt random movement.

Regarding temperature, its effect can only appear through the infection probability p (see formula (6)). Note that the effect of NDVI also appears through the movement of rodents (which influences the probability of encounter). In the model, the simulations show that NDVI has a more dominant effect than temperature. Moreover, in the second scenario, we noticed that the effect of temperature is observed in the fluctuations in Fig. 8a and Fig. 8b. Additionally, when NDVI

increases, the prevalence decreases (Fig. 8).

This result was also observed by Shirzadi et al. (2015) and Shiravand et al. (2018), which showed that the incidence of leishmaniasis increased in areas where vegetation coverage was low. In the same context, Mollalo et al. (2014) showed that the decrease of the vegetation cover is accompanied by increase of epidemic occurrence and vice versa.

The prevalence and rodents strategies that provides closest results to those observed in the field, are when the rodents movement is thoughtful and when $NDVI = NDVI_{max}$ (Ghawar et al., 2011).

Moreover, figure 9 demonstrated that the thoughtful movement is similar to the field rodents motion. These results are consistent with Rajabi et al. (2018). The latter found that rodents adapt their direction and movement depending on food suitability and availability. Field observation of Ghawar et al. (2015) showed that the higher vegetation cover is, the more new actives burrows are detected, indicating that *M.shawi* is able to assess the vegetation abundance.

Even though relevant findings are reported in this current study, a more comprehensive multispecies model which includes human and sandflies parameters would provide a deeper understanding of the ZCL transmission cycle. The lack of data on sandfly densities in Tunisia and on its association with plant density (NDVI) makes such the achievement of such study currently difficult. Moreover, no studies have been conducted on the demographic processes (births, deaths) in rodent reservoirs.

Other climatic factors, such as rainfall and humidity, which influence the transmission of ZCL are also important. However, in our case, these data were insufficient; thus, we used NDVI as an environmental factor (which depends on rainfall and humidity). It can be used when climate data as well as environmental characteristics of the site are not available (Gaudart et al., 2009).

6. Conclusion

In conclusion, our study provides an overview of the effects of climate (*i.e.* temperature) and environmental (*i.e.* NDVI) parameters on the rodents movements in a limited geographical area by using an ABM in order to simulate the transmission of ZCL among rodents. We considered two types of rodents movement (random or thoughtful). We observed that NDVI has a more dominant effect than temperature, and the transmission of ZCL was increased by decreasing the value of NDVI.

The findings reported in this current study would improve comprehension of the ZCL spread dynamics in larger areas, and thus to be subsequently used to implement prevention and control strategies of the epidemic.

7. Acknowledgements

We thank Professor Afif Ben Salah and the *Department of Medical Epidemiology* for their support and for providing references and unpublished information about temperature and *M. shawi*. We would also like to show our gratitude to Dr Dhafer Laouini for his financial support.

References

Adamou-Djerbaoui, M., Denys, C., Chaba, H., Seid, M., Djelaila, Y., Labdelli, F., 2013. Étude Du Régime Alimentaire D'Un Rongeur Nuisible (Meriones Shawii Duvernoy, 1842, Mammalia, Rodentia) En Algérie. Lebanese Science Journal 14, 15.

Arenas, R., Torres-Guerrero, E., Quintanilla-Cedillo, M.R., Ruiz-Esmenjaud, J., 2017. Leishmaniasis: A review. F1000Research 6, 1–15. doi:doi: 10.12688/f1000research.11120.1.

Bacaër, N., Guernaoui, S., 2006. The epidemic threshold of vector-borne diseases with seasonality: The case of cutaneous leishmaniasis in Chichaoua, Morocco. Journal of Mathematical Biology 53, 421–436. doi:doi: 10.1007/s00285-006-0015-0.

Bellali, H., Talmoudi, K., Alaya, N.B., Mahfoudhi, M., Ennigrou, S., Chahed, M.K., 2017. Effect of temperature, rainfall and relative density of rodent reservoir hosts on zoonotic cutaneous leishmaniasis incidence in Central Tunisia. Asian Pacific Journal of Tropical Disease 7, 88–96. doi:doi: 10.12980/apjtd.7.2017D6-330.

Bellali, H., Talmoudi, K., Harizi, C., Ben Alaya, N., Chahed, M., 2019. Using Ecosystem Approach to Address Infection with Leishmania Major in Central Tunisia . Archives of Epidemiology 3. doi:doi: 10.29011/2577-2252.101028.

Ben Ismail, R., Gradoni, L., Gramiccia, M., Bettini, S., Ben Rachid, M., Garraoui, A., 1986. Epidemic cutaneous leishmaniasis in tunisia: biochemical characterization of parasites. Transactions of the Royal Society of Tropical Medicine and Hygiene 80, 669–670.

Bettaieb, J., Toumi, A., Chlif, S., Chelghaf, B., Boukthir, A., Gharbi, A., Ben Salah, A., 2014. Prevalence and determinants of Leishmania major infection in emerging and old foci in Tunisia. Parasites and Vectors 7, 1–8. doi:doi: 10.1186/1756-3305-7-386.

Burattini, M.N., Coutinho, F.A., Lopez, L.F., Massad, E., 1998. Modelling the dynamics of leishmaniasis considering human, animal host and vector populations. Journal of Biological Systems 6, 337–356. doi:doi: 10.1142/S0218339098000224.

Cariboni, J., Gatelli, D., Liska, R., Saltelli, A., 2007. The role of sensitivity analysis in ecological modelling. Ecological modelling 203, 167–182.

Carpenter, J., Hasibeder, G., Dye, C., Carpenter, J., 1992. Mathematical modelling and theory for estimating the basic reproduction number of canine leishmaniasis. Parasitology 105, 43–53. doi:doi: 10.1017/S0031182000073674.

Chaves, L.F., Hernandez, M.J., 2004. Mathematical modelling of American Cutaneous Leishmaniasis: Incidental hosts and threshold conditions for infection persistence. Acta Tropica 92, 245–252. doi:doi: 10.1016/j.actatropica.2004.08.004.

Chidodo, D.J., Kimaro, D.N., Hieronimo, P., Makundi, R.H., Isabirye, M., Leirs, H., Massawe, A.W., Mdangi, M.E., Kifumba, D., Mulungu, L.S., 2020. Application of normalized difference vegetation index (ndvi) to forecast rodent population abundance in smallholder agro-ecosystems in semi-arid areas in tanzania. Mammalia 84, 136–143.

Chraiet-Rezgani, K., Bouafif-Ben Alaya, N., Habboul, Z., Hajjej, Y., Aoun, K., 2016. Aspects épidémiologiques et cliniques de la leishmaniose cutanée à Kairouan-Tunisie et particularités chez l'enfant. Bulletin de la Societe de Pathologie Exotique 109, 80–83. doi:doi: 10.1007/s13149-016-0475-4.

Clémence, L., 2009. La Leishmaniose Canine : ce que doit savoir le Pharmacien d ' officine. Ph.D. thesis. UNIVERSITE HENRI POINCARE - NANCY 1.

Daly, M., Daly, S., 1975. Behavior of psammomys obesus (rodenth: Gerbillinae) in the algerian sahara. Zeitschrift für Tierpsychologie 37, 298–321.

Dedet, J.P., 2009. Leishmanies, leishmanioses : biologie, clinique et thérapeutique. EMC - Maladies infectieuses 6, 1–14. URL:

http://dx.doi.org/10.1016/S1166-8598(09)50129-9, doi:doi: 10.1016/s1166-8598(09)50129-9.

Duan, W., Fan, Z., Zhang, P., Guo, G., Qiu, X., 2015. Mathematical and computational approaches to epidemic modeling: a comprehensive review. Frontiers of Computer Science 9, 806–826.

Garni, R., Tran, A., Guis, H., Baldet, T., Benallal, K., Boubidi, S., Harrat, Z., 2014. Remote sensing, land cover changes, and vector-borne diseases: Use of high spatial resolution satellite imagery to map the risk of occurrence of cutaneous leishmaniasis in Ghardaïa, Algeria. Infection, Genetics and Evolution 28, 725–734. URL: http://dx.doi.org/10.1016/j.meegid.2014.09.036, doi:doi: 10.1016/j.meegid.2014.09.036.

Gaudart, J., Touré, O., Dessay, N., lassane Dicko, A., Ranque, S., Forest, L., Demongeot, J., Doumbo, O.K., 2009. Modelling malaria incidence with environmental dependency in a locality of sudanese savannah area, mali. Malaria journal 8, 61.

Ghawar, W., Toumi, A., Snoussi, M.A., Chlif, S., Zĝatour, A., Boukthir, A., Bel Haj Hamida, N., Chemkhi, J., Diouani, M.F., Ben, S.A., 2011. Leishmania major infection among psammomys obesus and meriones shawi: Reservoirs of zoonotic cutaneous leishmaniasis in sidi bouzid (Central Tunisia). Vector-Borne and Zoonotic Diseases 11, 1561–1568. doi:doi: 10.1089/vbz.2011.0712.

Ghawar, W., Zaätour, W., Chlif, S., Bettaieb, J., Chelghaf, B., Snoussi, M.A., Salah, A.B., 2015. Spatiotemporal dispersal of meriones shawi estimated by radio-telemetry. International Journal of Multidisciplinary Research and Development 2, 211–216. URL: www.allsubjectjournal.com.

Gholamrezaei, M., Mohebali, M., Hanafi-Bojd, A.A., Sedaghat, M.M., Shirzadi, M.R., 2016. Ecological Niche Modeling of main reservoir hosts of zoonotic cutaneous leishmaniasis in Iran. Acta Tropica 160, 44–52. URL: http://dx.doi.org/10.1016/j.actatropica.2016.04.014, doi:doi: 10.1016/j.actatropica.2016.04.014.

Grignard, A., 2015. Modèles de visualisation à base d'agents. Ph.D. thesis. Paris 6.

Grimm, V., Berger, U., Bastiansen, F., Eliassen, S., Ginot, V., Giske, J., Goss-Custard, J., Grand, T., Heinz, S.K., Huse, G., Huth, A., Jepsen, J.U., Jørgensen, C., Mooij, W.M., Müller, B., Pe'er, G., Piou, C., Railsback, S.F., Robbins, A.M., Robbins, M.M., Rossmanith, E., Rüger, N., Strand, E., Souissi, S., Stillman, R.A., Vabø, R., Visser, U., DeAngelis, D.L., 2006. A standard protocol for describing individual-based and agent-based models. Ecological Modelling 198, 115–126. doi:doi: 10.1016/j.ecolmodel.2006.04.023.

Grimm, V., Berger, U., DeAngelis, D.L., Polhill, J.G., Giske, J., Railsback, S.F., 2010. The ODD protocol: A review and first update. Ecological Modelling 221, 2760–2768. URL: http://linkinghub.elsevier.com/retrieve/pii/S030438001000414X, doi:doi: 10.1016/j.ecolmodel.2010.08.019.

Hamidi, K., Mohammadi, S., Eskandarzadeh, N., 2018. How will climate change affect the temporal and spatial distributions of a reservoir host, the indian gerbil (tatera indica), and the spread of zoonotic diseases that it carries? Evolutionary Ecology Research 19, 215–226.

Hanafi-Bojd, A.A., Rassi, Y., Yaghoobi-Ershadi, M.R., Haghdoost, A.A., Akhavan, A.A., Charrahy, Z., Karimi, A., 2015. Predicted Distribution of Visceral Leishmaniasis Vectors (Diptera: Psychodidae; Phlebotominae) in Iran: A Niche Model Study. Zoonoses and Public Health 62, 644–654. doi:doi: 10.1111/zph.12202.

Hunter, E., MacNamee, B., Kelleher, J., 2018. A comparison of agent-based models and equation based models for infectious disease epidemiology. CEUR Workshop Proceedings 2259, 33–44.

Killick-Kendrick, R., 1999. The biology and control of phlebotomine sand flies. Clinics in dermatology 17, 279–289.

Koch, L.K., Kochmann, J., Klimpel, S., Cunze, S., 2017. Modeling the climatic suitability of leishmaniasis vector species in Europe. Scientific Reports 7, 1–10. URL: http://dx.doi.org/10.1038/s41598-017-13822-1, doi:doi: 10.1038/s41598-017-13822-1.

Marilleau, N., Lang, C., Giraudoux, P., 2018. Coupling agent-based with equation-based models to study spatially explicit megapopulation dynamics. Ecological Modelling 384, 34–42. URL:

https://doi.org/10.1016/j.ecolmodel.2018.06.011, doi:doi: 10.1016/j.ecolmodel.2018.06.011.

Marstona, C., Armitagea, R., Dansona, F., Giraudouxb, P., Ramireza, A., Craiga, P., 2007. Spatio-temporal modelling of small mammal distributions using modis ndvi time-series data. Authority Files for ISPRS .

Mejhed, H., Boussa, S., Mejhed, N.E.H., 2009. Development of mathematical models predicting the density of vectors: case of sandflies vectors of leishmaniasis, in: Proceedings of the 10th WSEAS international conference on Mathematics and computers in biology and chemistry, pp. 62–67.

Mollalo, A., Alimohammadi, A., Shahrisvand, M., Shirzadi, M.R., Malek, M.R., 2014. Spatial and statistical analyses of the relations between vegetation cover and incidence of cutaneous leishmaniasis in an endemic province, northeast of iran. Asian Pacific journal of tropical disease 4, 176–180.

Mollalo, A., Alimohammadi, A., Shirzadi, M.R., Malek, M.R., 2015. Geographic information system-based analysis of the spatial and spatio-temporal distribution of zoonotic cutaneous leishmaniasis in golestan province, North-East of Iran. Zoonoses and Public Health 62, 18–28. doi:doi: 10.1111/zph.12109.

Mollalo, A., Sadeghian, A., Israel, G.D., Rashidi, P., Sofizadeh, A., Glass, G.E., 2018. Machine learning approaches in gis-based ecological modeling of the sand fly phlebotomus papatasi, a vector of zoonotic cutaneous leishmaniasis in golestan province, iran. Acta tropica 188, 187–194.

Nadeem, F., Zamir, M., Tridane, A., Khan, Y., 2019. Modeling and control of zoonotic cutaneous leishmaniasis. Journal of Mathematics (ISSN 1016-2526) 51, 105–121.

Rajabi, M., Mansourian, A., Pilesjö, P., Shirzadi, M.R., Fadaei, R., Ramazanpour, J., 2018. A spatially explicit agent-based simulation model of a reservoir host of cutaneous leishmaniasis, Rhombomys opimus. Ecological Modelling 370, 33–49. URL: http://dx.doi.org/10.1016/j.ecolmodel.2017.12.004, doi:doi: 10.1016/j.ecolmodel.2017.12.004.

Rajabi, M., Pilesjö, P., Shirzadi, M.R., Fadaei, R., Mansourian, A., 2016. A spatially explicit agent-based modeling approach for the spread of Cutaneous

Leishmaniasis disease in central Iran, Isfahan. Environmental Modelling and Software 82, 330–346. doi:doi: 10.1016/j.envsoft.2016.04.006.

Roy, P.K., Biswas, D., Basir, F., 2015. Transmission dynamics of cutaneous leishmaniasis: a delay-induced mathematical study. Journal of Medical Research and Development 4, 11–23.

Saltelli, A., Ratto, M., Andres, T., Campolongo, F., Cariboni, J., Gatelli, D., Saisana, M., Tarantola, S., 2008. Global sensitivity analysis: The primer. john wiley & sons. Chichester, UK, ISBN 978&0&470&05997&S .

Shiravand, B., Hanafi-Bojd, A., Tafti, A.D., Abai, M., Almodarresi, A., Mirzaei, M., 2019. Climate change and potential distribution of zoonotic cutaneous leishmaniasis in Central Iran: Horizon 2030 and 2050. Asian Pacific Journal of Tropical Medicine 12, 204. URL: http://www.apjtm.org/text.asp?2019/12/5/204/259241, doi:doi: 10.4103/1995-7645.259241.

Shiravand, B., Tafti, A.A.D., Hanafi-Bojd, A.A., Almodaresi, S.A., Mirzaei, M., Abai, M.R., 2018. Modeling spatial risk of zoonotic cutaneous leishmaniasis in Central Iran. Acta Tropica 185, 327–335. doi:doi: 10.1016/j.actatropica.2018.06.015.

Shirzadi, M.R., Mollalo, A., Yaghoobi-Ershadi, M.R., 2015. Dynamic relations between incidence of zoonotic cutaneous leishmaniasis and climatic factors in golestan province, iran. Journal of arthropod-borne diseases 9, 148.

Stenseth, N., 1999. Population cycles in voles and lemmings: density dependence and phase dependence in a stochastic world. Oikos , 427–461.

Stenseth, N., 2003. Mice and rats: the dynamics and bioeconomics of agricultural rodents pests. Front Ecol Environ 1, 1–12.

Tabasi, M., Alesheikh, A., 2019. Development of an agent-based model for simulation of the spatiotemporal spread of leishmaniasis in gis (case study: Maraveh tappeh). Journal of Geomatics Science and Technology 8, 113–131.

Tabasi, M., Alesheikh, A.A., Sofizadeh, A., Saeidian, B., Pradhan, B., AlAmri, A., 2020. A spatio-temporal agent-based approach for modeling the spread of zoonotic cutaneous leishmaniasis in northeast iran. Parasites & Vectors 13, 1–17.

Taillandier, P., Gaudou, B., Grignard, A., Huynh, Q.N., Marilleau, N., Caillou, P., Philippon, D., Drogoul, A., 2019. Building, composing and experimenting complex spatial models with the gama platform. GeoInformatica 23, 299–322.

Talmoudi, K., Bellali, H., Ben-Alaya, N., Saez, M., Malouche, D., Chahed, M.K., 2017. Modeling zoonotic cutaneous leishmaniasis incidence in central Tunisia from 2009-2015: Forecasting models using climate variables as predictors. PLoS Neglected Tropical Diseases 11, 1–18. doi:doi: 10.1371/journal.pntd.0005844.

Taylor, L.H., Latham, S.M., Woolhouse, M.E., 2001. Risk factors for human disease emergence. Philosophical Transactions of the Royal Society B: Biological Sciences 356, 983–989. doi:doi: 10.1098/rstb.2001.0888.

Toumi, A., Chlif, S., Bettaieb, J., Alaya, N.B., Boukthir, A., Ahmadi, Z.E., Salah, A.B., 2012. Temporal dynamics and impact of climate factors on the incidence of Zoonotic Cutaneous Leishmaniasis in central Tunisia. PLoS Neglected Tropical Diseases 6, 0–7. doi:doi: 10.1371/journal.pntd.0001633.

Treuil, J.P., Drogoul, A., Zucker, J.D., 2008. Modélisation et simulation à base d'agents: exemples commentés, outils informatiques et questions théoriques. Dunod.

Wang, J., Rich, P.M., Price, K.P., 2003. Temporal responses of ndvi to precipitation and temperature in the central great plains, usa. International journal of remote sensing 24, 2345–2364.

Zilberstein, D., Shapira, M., 1994. The role of ph and temperature in the development of leishmania parasites. Annual review of microbiology 48, 449–471.